

*Spatio-temporal assessment of streamflow
droughts over Southern South America:
1961–2006*

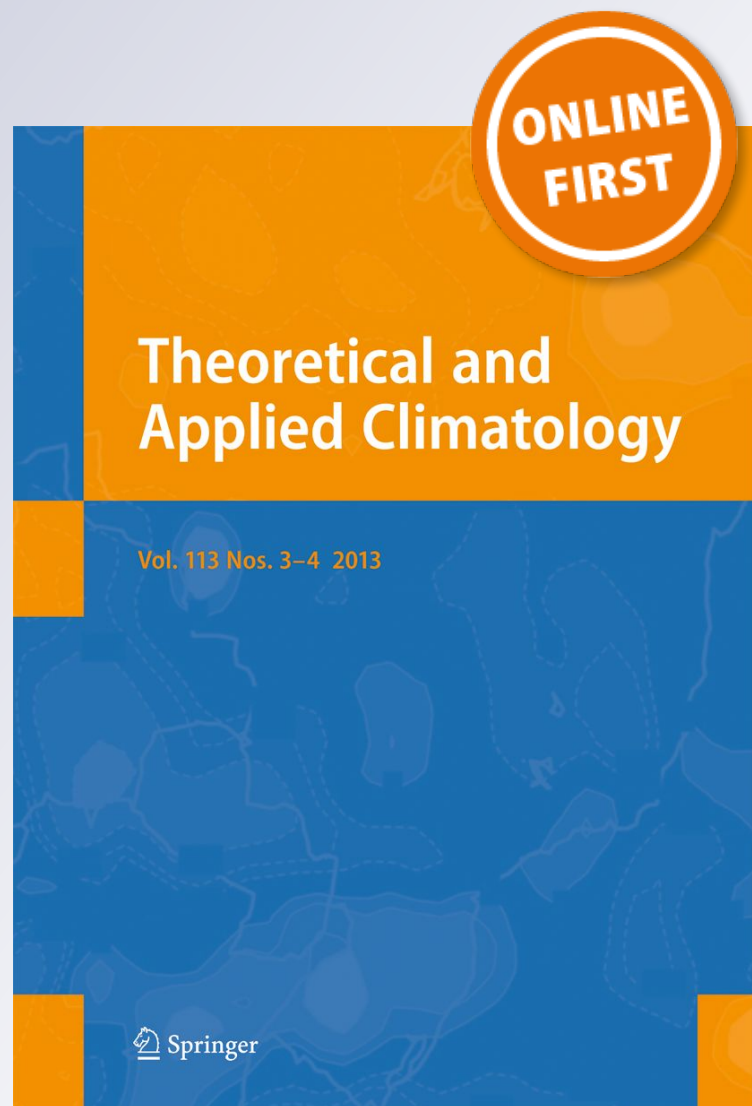
Juan Antonio Rivera & Olga C. Penalba

Theoretical and Applied Climatology

ISSN 0177-798X

Theor Appl Climatol

DOI 10.1007/s00704-017-2243-1



Your article is protected by copyright and all rights are held exclusively by Springer-Verlag GmbH Austria. This e-offprint is for personal use only and shall not be self-archived in electronic repositories. If you wish to self-archive your article, please use the accepted manuscript version for posting on your own website. You may further deposit the accepted manuscript version in any repository, provided it is only made publicly available 12 months after official publication or later and provided acknowledgement is given to the original source of publication and a link is inserted to the published article on Springer's website. The link must be accompanied by the following text: "The final publication is available at link.springer.com".

Spatio-temporal assessment of streamflow droughts over Southern South America: 1961–2006

Juan Antonio Rivera^{1,2}  · Olga C. Penalba^{3,4}

Received: 7 October 2016 / Accepted: 2 August 2017
© Springer-Verlag GmbH Austria 2017

Abstract This paper performed a streamflow drought climatology considering some of the most important rivers of Southern South America, a region highly vulnerable to climatic variations, based on the analysis of monthly streamflow records. The standardized hydrological drought index (SHDI) was used in order to depict the main characteristics of droughts—number of drought events, mean duration, and mean severity—over the period 1961–2006. Firstly, the suitability of this index based on the two-parameter gamma distribution was evaluated, considering that the use of the SHDI has been limited over the region. The regional aspects of streamflow droughts were identified through a clear relationship between drought frequency and its duration, indicating different temporal variations in streamflow records over the study area. Spatial patterns exhibit heterogeneous features in terms of streamflow drought severity and can be associated to the geographical characteristics of the basins. Observed trends in the SSI are in line with the increases in precipitation totals over the second half of the twentieth century over much of the

study area. Nevertheless, drought conditions are observed more often in the basins south of 40°S, in line with recent trends in large-scale climatic oscillations. The streamflow drought characteristics can provide critical values for different water-based activities, as also information to develop strategic plans that are needed for adequate water resource management considering the different climatic features over Southern South America.

Keywords Streamflow droughts · Temporal variability · Water resources

1 Introduction

Extreme hydrometeorological events are one of the most costly disasters in Southern South America (SSA), a region that is prone to experience prolonged drought events and flooding episodes that can even generate human losses (Cavalcanti et al. 2015; Carril et al. 2016). Droughts are one of the least understood natural disasters, with multiple regional aspects that highlight the vulnerability of societies (Shiferaw et al. 2014; Wilhite et al. 2014). Particularly, SSA experienced large-scale droughts during the years 1962, 1965/1966, 1971/1972, 1988/1989, 1995/1996, and 2008/2009 (Rivera and Penalba 2014). The propagation of a precipitation deficit through the hydrological cycle may eventually lead to hydrological droughts, characterized by abnormally low streamflow in rivers and low levels in lakes, reservoirs, and groundwater (Feyen and Dankers 2009, Wong et al. 2013). The hydropower generation, the fluvial transportation, the irrigation for agricultural activities, and the availability of water for human have significant consequences in periods with hydrological drought conditions. Within SSA, the La Plata Basin (LPB) stands out as one of the largest basins in the world, with a

✉ Juan Antonio Rivera
jrivera@mendoza-conicet.gob.ar

- ¹ Instituto Argentino de Nivología, Glaciología y Ciencias Ambientales (IANIGLA), Av. Ruiz Leal s/n, Parque General San Martín, 5500 Mendoza, Argentina
- ² Universidad Juan Agustín Maza, Av. Acceso Este, Lateral Sur 2245, Guaymallén, 5519 Mendoza, Argentina
- ³ Departamento de Ciencias de la Atmósfera y los Océanos, Facultad de Ciencias Exactas y Naturales, Universidad de Buenos Aires, Intendente Güiraldes 2160, Pabellón 2, 2° Piso – Ciudad Universitaria, C1428EGA Buenos Aires, Argentina
- ⁴ Consejo Nacional de Investigaciones Científicas y Técnicas (CONICET), Av. Rivadavia 1917, C1033AAJ Buenos Aires, Argentina

hydropower generation that represents the 76% of the total generated hydropower of Argentina, Bolivia, Brazil, Paraguay, and Uruguay (Cuya et al. 2013). On the other hand, small basins located over the semi-arid Central Andes, where streamflows are mostly originated by snowmelt contributions during the warm season, are the key for sustaining agricultural oases that fed its almost 2.5 million inhabitants (Rivera et al. 2017a).

The knowledge about hydrological drought over SSA has several gaps and uncertainties regarding the regional differences among the basins and the methodologies used to define this extreme phenomenon. Hydrological drought indices were based largely on streamflow, as this variable summarizes and is the by-product of essentially every hydrometeorological process taking place in watersheds and river basins (Heim 2002). In this sense, hydrological droughts are usually studied through streamflow droughts, defined as periods where the streamflow levels are below a predetermined truncation level. Fernández-Larrañaga (1997) characterized streamflow drought events in the central Chile in terms of several levels of annual demand. This study was extended to the basins located in the central-west region of Argentina (Fernández and Buscemi 2000) with similar results in terms of temporal occurrences of streamflow droughts, in part as a consequence of the role of snowmelt as regulator of streamflows over the Central Andes. Díaz et al. (2016) defined a yearly threshold and expanded the analysis to 14 basins in the central-west and northwest regions of Argentina, identifying the occurrence of multiannual droughts mainly during 1956–1976. Nevertheless, as stated in Vicente-Serrano et al. (2012), given the contrasting river regimes and flow magnitudes that can occur among neighboring basins, the spatial comparison of drought severity and the development of drought maps are impossible when using the method of runs. Recent research over SSA considered the seasonality of streamflows by using annual indices based on the number of days with low flows and its standardized cumulative deficit (Rivera et al. 2017a, b) allowing to identify low-frequency variations of streamflow drought characteristics and its relationship with climate variability over central-west Argentina and Patagonia.

During recent years, standardized drought indices have received special attention due its multiple advantages over other indices. Particularly, the standardized precipitation index (SPI, McKee et al. 1993) has been recommended by the World Meteorological Organization (WMO) as a reference drought index that should be used by national meteorological and hydrological services worldwide to characterize meteorological droughts (Hayes et al. 2011). The SPI has been adopted as an operational drought monitoring tool by the national weather services of Argentina (Servicio Meteorológico Nacional), Brazil (Instituto Nacional de Meteorologia), Chile (Dirección Meteorológica de Chile), Paraguay (Dirección de Meteorología e Hidrología), and Uruguay (Instituto Uruguayo

de Meteorología). McKee et al. (1993) suggested that usable water sources to identify drought conditions include soil moisture, groundwater, snowpack, streamflow, and reservoir storage. Therefore, using monthly streamflow data as input, Dehghani et al. (2014) proposed the standardized hydrological index (SHDI) as a streamflow drought indicator to make spatial and temporal comparisons over a wide variety of river regimes and flow characteristics. Similar to the SPI, the SHDI has a number of advantages, as its simplicity and flexibility. The standardization process allows the comparison among streamflows from different regions and basins. Moreover, because of its normal distribution, the frequencies of the extreme and severe droughts for any location and any timescale are comparable (Dehghani et al. 2014). Few studies used standardized indices to assess streamflow drought conditions over SSA. Bianchi et al. (2017) used the standardized runoff index (SRI, Shukla and Wood 2008) to identify relationships between the size of Llanquanelo lake—located in central-western Argentina—and the input streamflows over its basin. Núñez et al. (2014) analyzed the effect of multidecadal variability on the applicability of the standardized streamflow index (SSI, Vicente-Serrano et al. 2012) over north-central Chile. On the other hand, the use of standardized indices was widely applied in several regions of the world to depict streamflow drought conditions, like in Italy (Soláková et al. 2014), Spain (Vicente-Serrano et al. 2012), Iran (Tabari et al. 2013), and UK (Barker et al. 2016, Svensson et al. 2017) among others.

There is a lack of studies comparing streamflow conditions on a regional perspective over SSA, a task that needs to be performed considering appropriate methodologies and indices given the different streamflow regimes over the region. In this sense, the objective of this research is to broaden the application of the SHDI to some of the largest basins over SSA in order to depict the main characteristics of streamflow droughts over the region. Considering the acceptability obtained by the SPI during recent years over SSA, it is expected that the SHDI results and its interpretability likely to be familiar to meteorological and hydrological agencies, water managers, and scientists focused on drought research and monitoring. An assessment of streamflow drought characteristics over SSA can provide critical values for different water based activities, as also information to develop strategic short- and long-term plans that are needed for adequate water resource management. Understanding the temporal variabilities of streamflow drought characteristics and its regional patterns is relevant for decision-making processes regarding water distribution for irrigation and human consumption, hydropower generation, and environmental flows. Given that the analyzed basins generate a large proportion of the total hydroelectric power of Argentina, Brazil, Paraguay, and Uruguay, it is expected that the

results obtained regarding streamflow drought characteristics and its different temporal variabilities have direct application for water resources management over the region.

2 Data and methods

2.1 Study area and data base

Monthly streamflow records from 53 gauging stations located in SSA, between 18°S and 50°S (Fig. 1a), were obtained from the Hydrological Data Base belonging to the Water Resources Agency of Argentina (<http://bdhi.hidricosargentina.gov.ar/>) and the CLARIS LPB Data Base (Penalba et al. 2014). The study area comprises some of the main basins of Argentina, Brazil, Chile, Paraguay, and Uruguay. There is a wide spectrum of climatic regions within SSA, arising from the long meridional span of the continent and its prominent orography (Fig. 1b), which led to diverse patterns of weather and climate (Garreaud et al. 2009). These features are responsible for the annual precipitation patterns (Fig. 1c) and drive the vast diversity of hydrologic characteristics over SSA. In this sense, Table 1 shows some statistical—mean monthly streamflow value, specific streamflow, coefficient of variation (cv), coefficient of skewness (cs), lag-one correlation coefficient (ρ_1)

—and geographical—location, altitude, area—characteristics of the streamflow series. The diversity in the flow regimes is evident in the cv values, ranging from 0.25 to 1.37. Moreover, mean streamflow values range from less than $10 \text{ m}^3/\text{s}$ in small semi-arid basins of Patagonia (Atlantic South Coast and Negro Basin) and Central Andes (Colorado Basin) to over $18,000 \text{ m}^3/\text{s}$ over Paraná river (LPB).

A common period between 1961 and 2006 was considered to obtain the main features of streamflow droughts based on data availability and quality. The need for data infilling was minimal, given that the selected stations have less than 3% of missing data. Several infilling methods were applied, depending on the size of the gap, the hydrological conditions at the site when the gap occurred, and the availability of nearby gauging stations, following the recommendations made by World Meteorological Organization (WMO) (2008). Additionally, a homogeneity control using the Standard Normal Homogeneity Test (Alexandersson 1986) allowed to identify inhomogeneities in 18 time series. These inhomogeneities were not corrected given that correspond to climatic jumps and not to instrumental factors or data errors. This was verified analyzing the spatial distribution of the dates of the changes (not shown) and also comparing the results with previous findings over the studied area (Vich et al. 2014). It is worthwhile to mention that, even when some regions over the study area are characterized by an arid to semi-arid climate,

Fig. 1 a Location of the study area, its main basins, and the spatial distribution of the analyzed hydrological stations; (b) the main orographic features of the region; and (c) the mean annual rainfall

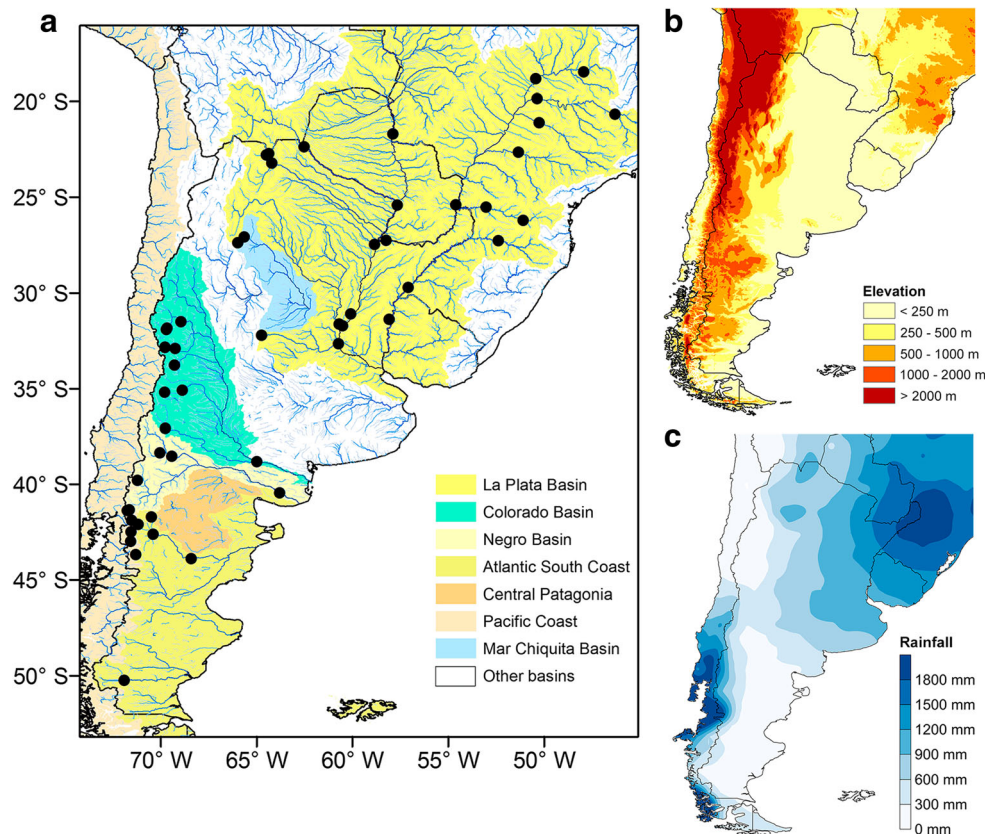


Table 1 Geographical characteristics of the selected stations and statistical properties of monthly streamflows

ID	River	Station name	Lat (°S)	Lon (°W)	Altitude (masl)	Drainage area (km ²)	Mean monthly streamflow (m ³ /s)	Specific streamflow (l/s km ²)	<i>cv</i>	<i>cs</i>	ρ_I
1	Grande	Furnas	20,67	46,30	540	25,650	94,9	3,7	0,67	1,46	0,73
2	Uruguay	Salto Grande	31,38	58,08	11	36,827	5215,1	23,3	0,76	1,39	0,58
3	Las Cañas	Potrero del Clavillo	27,40	65,97	1300	1000	3,8	3,8	0,96	2,41	0,57
4	Los Sosa	RP N° 307 Km 19	27,10	65,64	610	620	5,0	8,1	1,03	2,45	0,63
5	Grande	Água Vermelha	19,86	50,36	350	139,000	2171,7	15,6	0,60	1,26	0,76
6	Paranaíba	Emborcacao	18,47	47,93	530	29,300	485,0	16,6	0,76	1,58	0,71
7	Alegre	Sao Simao	18,83	50,43	330	171,000	2527,7	14,8	0,63	1,24	0,76
8	Parapanema	Capivara	22,66	51,34	285	85,000	1206,8	14,2	0,61	2,68	0,52
9	Iguazú	Salto Osorio	25,54	53,03	330	55,000	1136,5	20,7	0,75	2,44	0,48
10	Uruguay	Itá	27,28	52,38	265	44,500	1115,1	25,1	0,84	2,55	0,46
11	Bermejo	Aguas Blancas	22,73	64,36	405	4850	93,7	19,3	1,15	1,94	0,61
12	Pescado	Cuatro Cedros	22,80	64,48	450	1700	51,8	30,5	1,16	2,00	0,61
13	Pilcomayo	La Paz	22,38	62,52	230	96,000	208,6	2,2	1,32	2,39	0,62
14	Bermejo	Pozo Sarmiento	23,22	64,20	327	25,000	392,5	15,7	1,19	2,15	0,61
15	de los Patos	Alvarez Condarco	31,92	69,70	1923	3710	20,5	5,5	1,03	2,53	0,79
16	de los Patos	La Plateada	31,86	69,66	1870	8500	47,2	5,6	1,15	3,14	0,79
17	San Juan	KM 47,3	31,52	68,94	934	25,670	61,0	2,4	0,87	3,00	0,81
18	Atuel	La Angostura	35,10	68,87	1302	3800	36,7	9,7	0,55	1,88	0,80
19	Cuevas	Punta de Vacas	32,87	69,77	2406	680	7,1	10,4	0,87	2,83	0,81
20	Mendoza	Guido	32,92	69,24	1408	8180	46,9	5,7	0,79	2,12	0,79
21	Salado	Cañada Ancha	35,20	69,78	1680	810	11,0	13,6	0,99	2,87	0,78
22	Tunuyán	Valle de Uco	33,78	69,27	1199	2380	29,8	12,5	0,80	1,92	0,80
23	Vacas	Punta de Vacas	32,85	69,76	2400	570	4,7	8,2	0,91	3,15	0,75
24	Colorado	Pichi Mahuida	38,82	64,98	122	22,300	129,5	5,8	0,71	1,81	0,79
25	Manso	Los Alerces	41,37	71,75	700	750	45,6	60,8	0,54	0,92	0,58
26	Manso	Los Moscos	41,35	71,64	795	580	34,8	60,0	0,52	0,95	0,57
27	Negro	Primera Angostura	40,46	63,79	32	95,000	789,7	8,3	0,53	0,94	0,78
28	Quemquemtreu	Escuela N° 139	41,90	71,50	409	650	9,4	14,5	0,57	1,28	0,63
29	Chico	Cerro Mesa	41,71	70,48	747	3404	7,8	2,3	1,37	2,83	0,66
30	Colorado	Buta Ranquil	37,08	69,75	850	15,300	153,5	10,0	0,76	1,91	0,78
31	Neuquen	Paso de Indios	38,53	69,41	498	30,843	304,9	9,9	0,74	0,97	0,67
32	Chimehuin	Naciente	39,79	71,21	875	790	65,6	83,0	0,60	0,76	0,67
33	Agrio	Bajada del Agrio	38,37	70,03	660	7300	76,6	10,5	0,70	1,04	0,67
34	Carrenleufú	La Elena	43,68	71,30	783	1500	33,6	22,4	0,40	0,60	0,67
35	Carrileufú	Cholila	42,50	71,54	532	580	49,3	85,0	0,51	1,89	0,41
36	Chubut	El Maiten	42,10	71,17	680	1200	20,0	16,7	0,71	1,16	0,59
37	Chubut	Los Altares	43,89	68,40	275	16,400	48,7	3,0	0,88	1,55	0,67
38	Gualjaina	Gualjaina	42,61	70,38	480	2800	14,8	5,3	0,93	1,61	0,64
39	Fontana	Estancia Amancay	42,99	71,56	627	47	1,5	31,9	0,73	1,65	0,55
40	Paraguay	Puerto Pilcomayo	25,42	57,65	63	800,000	3706,1	4,6	0,52	1,24	0,89
41	Santa Cruz	Charles Fuhr	50,25	71,91	206	15,550	703,0	45,2	0,51	0,69	0,83
42	Paraná	Túnel Subfluvial	31,72	60,52	17	2,302,000	15,198,3	6,6	0,29	0,70	0,83
43	San Javier	Helvecia	31,10	60,08	21	21,668	743,6	34,3	0,89	2,91	0,81

Table 1 (continued)

ID	River	Station name	Lat (°S)	Lon (°W)	Altitude (masl)	Drainage area (km ²)	Mean monthly streamflow (m ³ /s)	Specific streamflow (l/s km ²)	<i>cv</i>	<i>cs</i>	ρ_1
44	Paraná	Timbúes	32,66	60,73	12	2,346,000	16,906,2	7,2	0,25	0,16	0,86
45	Sistema Setúbal	La Guardia	31,63	60,68	17	26,587	1355,3	51,0	0,91	3,40	0,81
46	Uruguay	Paso de los Libres	29,72	57,08	40	189,000	4593,5	24,3	0,78	1,65	0,56
47	Paraná	Corrientes	27,48	58,83	52	1,950,000	18,180,4	9,3	0,36	1,56	0,78
48	Paraná	Itatí	27,27	58,24	59	1,600,000	13,359,5	8,3	0,34	1,54	0,74
49	Grande	Ume Pay	32,22	64,73	620	762	11,3	14,8	1,01	1,94	0,58
50	Tiete	Nova Avanhandava	21,12	50,25	325	70,500	805,8	11,4	0,60	1,87	0,66
51	Paraná	Itaipu	25,40	54,60	110	820,000	11,242,3	13,7	0,43	0,96	0,75
52	Iguazú	Uniao da Vitoria	26,23	51,08	750	24,000	509,2	21,2	0,75	2,21	0,50
53	Paraguay	Porto Murtinho	21,70	57,89	77	600,000	2422,9	4,0	0,46	0,72	0,93

cv coefficient of variation, *cs* coefficient of skewness, ρ_1 lag-one correlation coefficient

none of the analyzed rivers are intermittent or ephemeral, which guarantees a proper definition of drought events based on the SHDI.

2.2 Standardized hydrological drought index (SHDI)

Several standardized indices were developed during recent years considering streamflow data as input variable (e.g., Standardized Runoff Index (SRI), Shukla and Wood 2008; Streamflow Drought Index (SDI), Nalbantis and Tsakiris 2009; Standardized Inflow Index (SQI), Amor et al. 2009). In order to define the streamflow drought occurrences, we used the SHDI (Dehghani et al. 2014), a widely used index being an extension from the SPI to depict hydrologic aspects of drought. In this sense, the SHDI quantifies the number of standard deviations that the streamflow deviates from the climatological average of a location, by transforming monthly streamflows into *z*-scores. The procedure for calculating the SHDI is analogue to the SPI; therefore, the selection of a suitable probability density function that adequately fit the monthly streamflows summed over the time scale of interest is a key aspect in the calculation. This is performed separately for each month of the year and for each location in space. Each probability density function is then transformed into the standard normal distribution ($\mu = 0$, $\sigma = 1$) (Lloyd-Hughes and Saunders 2002). In this study, the SHDI was calculated on time scale of 1 month; nevertheless, the index can be calculated on any time scale, i.e., accumulating streamflow monthly data over 1, 3, 6, 12, or 24 months. The reader can find a detailed description of the calculation of the SPI in Lloyd-Hughes and Saunders (2002), changing precipitation with streamflow as input data to obtain the SHDI. Given that no ephemeral or intermittent rivers were considered for the

streamflow drought assessment, there is no need to include the relative frequency of streamflow containing zero values for the cumulative density function, a procedure that is common when analyzing precipitation data.

2.3 Distribution fitting

The first step in calculating the SHDI is to determine a probability density function that describes the long-term time series of streamflow observations. Generally, streamflow may possess a skewed probability distribution which can well be approximated by the family of the gamma distribution functions (Nalbantis and Tsakiris 2009). Table 1 confirms that all the selected rivers have positive *cs*, suggesting that the two-parameter gamma (GA) distribution could be adequate over the study area. Shukla and Wood (2008) showed that the GA distribution performed well fitting streamflow records over the USA, highlighting a better performance for low runoff values in comparison with the two-parameter lognormal distribution. Dehghani et al. (2014) compared five different probability distributions—normal, lognormal, exponential, GA, and log-gamma—showing that among all functions gamma showed the best fit. In this sense, given the different hydroclimatic features over SSA, a proper evaluation of the suitability of the GA distribution is necessary prior to the calculation of the SHDI. At this point, it is worthwhile to clarify that we are not intended to make a comparison among different probability distributions, a task that was correctly performed by Vicente-Serrano et al. (2012) and Núñez et al. (2014), among others. In this sense, any probability distribution used is no more than an approximation to the observed streamflow data, and there is no single distribution that “best” fit the population of monthly streamflows at all stations.

Therefore, considering this simplification, we fitted the GA distribution to the monthly streamflow values and evaluated its suitability through the Anderson-Darling goodness-of-fit test (AD, Anderson and Darling 1952) for a confidence level of 95%. This test used a test statistic of the sum of squares of the differences between the empirical and theoretical distribution functions with a weight function that emphasized discrepancies in both tails (Shin et al. 2012). Several papers showed the supremacy of AD test against other typical tests as Cramer von Mises or Kolmogorov-Smirnov given its sensitivity to the differences in the tails of the distribution (Stephens 1976; Laio 2004; Shin et al. 2012), something that needs to be considered when extreme events are under analysis. We consider that at least 8 months of the year have to exhibit significant fits to the GA distribution in order to use the streamflow series to calculate the SHDI. Moreover, after the calculation of the SHDI, we analyzed if the selection of the GA distribution resulted in normally distributed SHDI series after the equi-probability transformation. This was assessed also through the AD test.

2.4 Streamflow drought definition

A streamflow drought event was defined as the period when SHDI values are below -1.0 , which means that streamflow departures from average conditions exceed one standard deviation. This allowed the identification of the onset and end of the drought event and other commonly used statistics, as (i) the number of drought events (NDE), (ii) the mean drought duration (MDD, average duration of all drought events), and (iii) the mean drought severity (MDS, average SHDI values of all drought events). Three drought categories are usually used for streamflow drought assessment, based on the categories of the SPI (Lloyd-Hughes and Saunders 2002): moderate drought ($-1.5 < \text{SHDI} \leq -1.0$), severe drought ($-2.0 < \text{SHDI} \leq -1.5$), and extreme drought ($\text{SHDI} \leq -2.0$). The selection of these thresholds is in line with recent research based on streamflow records (Dehghani et al. 2014, Barker et al. 2016, Rangecroft et al. 2016) and will help to compare the results obtained considering meteorological drought assessment based on the SPI over SSA (e.g., Penalba and Rivera 2016).

2.5 Trends in the SHDI

The non-parametric Mann-Kendall statistical test has been recommended by the WMO to detect trends in hydrological time series, given that it is easy to calculate, insensitive to missing values, and it is able to identify any trend in a time series without specifying whether the trend is linear or non-linear (Wu et al. 2007a). Nevertheless, the limitations of this trend test are associated with the fact

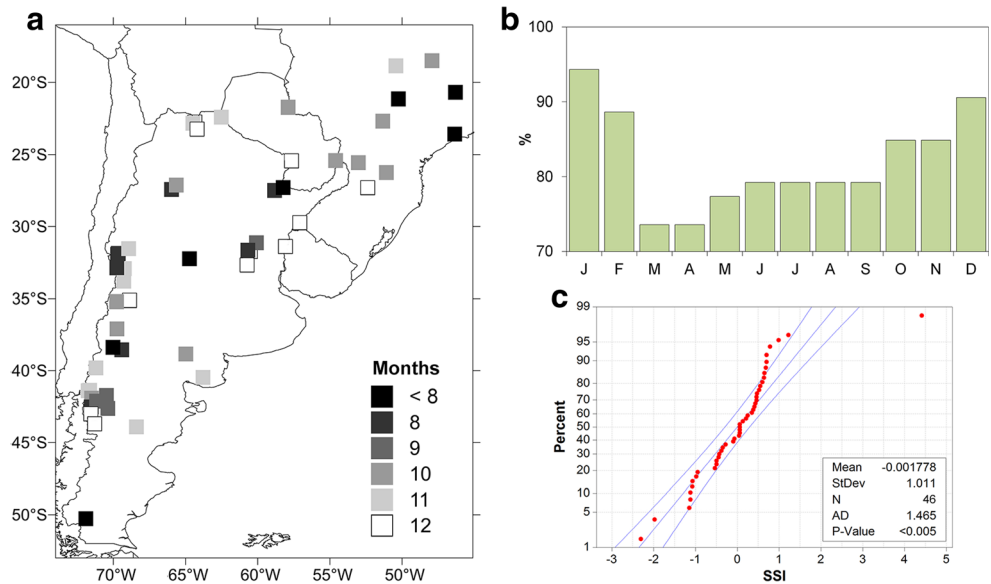
that it was originally designated for uncorrelated data, and most of the hydrometeorological variables exhibit significant serial correlation. Kulkarni and Von Storch (1995) reported that even a small serial correlations cause severe malfunctions of the Mann-Kendall test, increasing the probability of detecting a significant trend when actually none exist. In order to account for the presence of serial correlation, we applied the modified Mann-Kendall (MMK) test Hamed and Rao (1998) to identify trends in the SHDI time series. This decision is supported by the large values in the ρ_I (Table 1), which indicates a strong short-term persistence in the streamflow time series. The MMK test has been widely applied to detect the presence of trends in hydrometeorological time series (Andreadis and Lettenmaier 2006; Khaliq et al. 2009; Sousa et al. 2011; Zhang et al. 2012; Zhu et al. 2016). A detailed description of the test can be found in Hamed and Rao (1998). The statistical significance of upward/downward trends is evaluated at 90, 95, and 99% confidence levels.

3 Results

3.1 SHDI distribution fitting

From the 636 goodness-of-fit tests—12 months multiplied by 53 gauging stations—more than 82% of the cases showed significant fits to a GA distribution. The spatial distribution of the number of months with significant fits for each station shows a heterogeneous pattern (Fig. 2a). This characteristic typically differs from the results that can be obtained through the SPI, given that non-significant GA distribution fits tend to be located over arid to semi-arid regions where several months with zero precipitation values are recorded (Lloyd-Hughes and Saunders 2002; Wu et al. 2007b; Penalba and Rivera 2013). The annual cycle of the percentage of stations with significant fits to the GA probability distribution is shown in Fig. 2b. March and April are the months with higher failure ($> 25\%$), attributed to the stations of Colorado Basin and Patagonia (Negro Basin, Atlantic South Coast and Central Patagonia), respectively. On the other hand, January and December show rejection rates lower than 10% (Fig. 2b). As mentioned in previous section, we decided to remove from the analysis the stations with less than 8 months with significant fits to the GA distribution, which resulted to discard the following stations marked with black squares in Fig. 2a: Furnas, Agua Vermelha, Bajada del Agrio, Charles Führ, Itatí, Ume Pay, and Nova Avanhandava (see Table 1 for details). After discarding these time series, the significant fits increased to 87%, showing the suitability of the GA distribution in reproducing the monthly streamflow totals over SSA. Once the time series of SHDI were obtained, we analyzed for each month and station if the equi-probability transformation

Fig. 2 **a** Number of months with significant fits to the GA probability distribution (95% confidence level); **b** annual cycle of the percentage of stations with significant fits to the GA probability distribution; **c** an example of the normal distribution fit of January SHDI data from Santa Cruz river (station 41, see Table 1 for details)



resulted in normally distributed SHDI series. After this procedure, we obtained a spatial pattern similar to Fig. 2a, with an average rejection lower than 13% and a monthly distribution of significant fits more homogeneous (not shown). As an example of what kind of results can be expected by trying to obtain the SHDI using monthly streamflow time series that does not fit properly to a GA distribution—or whatever probability distribution selected—Fig. 2c illustrates the fit obtained from data of January from Santa Cruz river (station 41, see Table 1 for details). The points ideally have to follow the straight line of the center to guarantee a proper fit to a normal distribution. Nevertheless, several streamflow values are distributed outside the 95% confidence intervals, leading to a non-significant fit, evident in higher AD value and a *p* value lower than 0.05. As a result of this assessment, 46 stations will be used to calculate the streamflow drought characteristics based on the SHDI.

3.2 Streamflow drought characteristics

The streamflow drought characteristics, i.e., number of drought events, mean drought duration, and mean drought severity, for the SHDI obtained with the 46 selected stations during 1961–2006 are shown in Fig. 3. The NDE ranges from 20 to 50, indicating that there are regions where streamflow droughts are recorded approximately every year. Stations with larger NDE are located mostly over the eastern part of LPB—Uruguay river and upper Paraná river—and over the northwestern portion of Argentina. Lower values in the NDE are distributed along Colorado Basin stations, lower and middle Paraná river and Paraguay river (Fig. 3). The stations located south of 40°S show a heterogeneous pattern, with over 30 streamflow drought events in average for the 46 years of

study. The MDD values indicate that streamflow droughts usually last between 1 and 8 months, depending on the region considered. As previously shown in regional studies based on the threshold level method (Rivera et al. 2017a, b), there is an indirect relationship between drought frequency—NDE—and its duration: The stations with more (less) number of streamflow drought events have short (large) mean duration. This relationship indicates that higher-frequency variabilities are dominant in the time series of SHDI over eastern part of LPB, the northwestern portion of Argentina and some rivers of Patagonia region in comparison with the SHDI time series over the rivers belonging to Colorado Basin and Paraná and Paraguay rivers, which are characterized by lower-frequency variations. This is further illustrated in Fig. 4, where the SHDI time series of stations Álvarez Condarco and Paso de los Libres are shown. There are two factors that might contribute to the observed difference. One factor is that over eastern LPB annual precipitation cycle is not very marked. This is due to both convective activity in summer and winter precipitation as a result of transient activity that lead to a maximum of precipitation over Southern Brazil and Uruguay (Vera et al. 2002) and also due to the significant frequency of cyclogenesis during winter and spring (Gan and Rao 1991). These factors influence precipitation over LPB on intra-seasonal to seasonal time scales and contribute to the behavior observed in the SHDI, although interannual variations associated with El Niño-Southern Oscillation are also relevant (Penalba and Rivera 2016). The other factor may be associated with the interannual and interdecadal variations of the snowmelt contribution to streamflow in Colorado Basin and some basins south of 40°S (Masiokas et al. 2006). This effect can be responsible for the low-

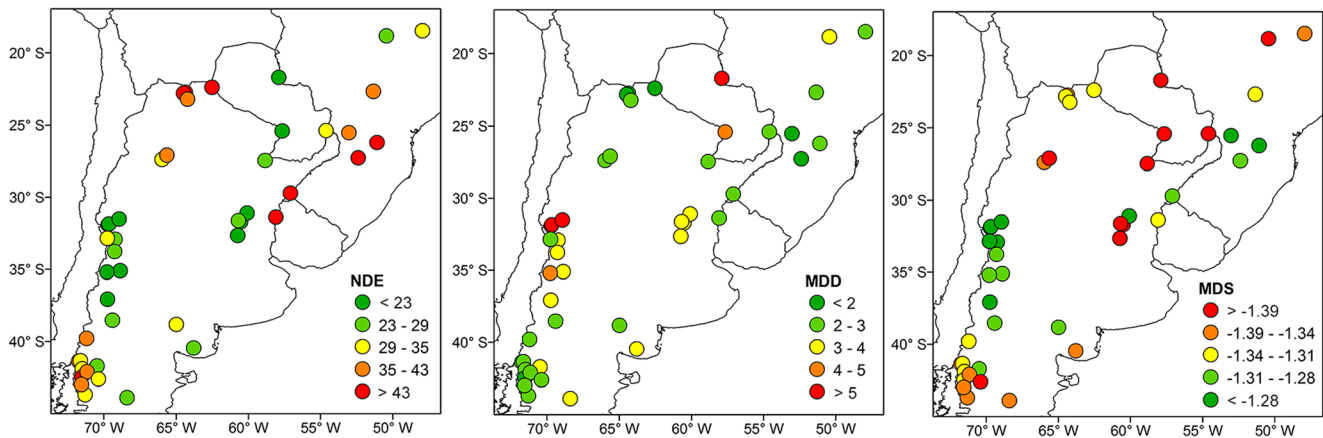


Fig. 3 Streamflow drought indicators for the selected stations: (*left*) number of drought events, NDE, in the period 1961–2006; (*center*) mean drought duration (MDD) (in months), and (*right*) mean drought severity (MDS) (in SHDI values)

frequency fluctuations observed in the SSI time series from station Álvarez Condarco, although for Patagonian basins rainfall plays a relevant role in modulating streamflow.

Regarding the streamflow drought severity, lower severity values are observed over Colorado Basin and in the eastern part of LPB. Conversely, larger MDS values are present in the rest of the LPB and in most of the rivers of Patagonia (south of 40°S) (Fig. 3). The MDS spatial distribution seems to be unrelated to either the NDE or the MDD, although when considering the accumulated severity, i.e., sum of the departures from the -1.0 threshold, large MDD can be attributed to large accumulated severity, i.e., large cumulative deficit volume.

Comparing this streamflow drought climatology with the climatology of meteorological droughts for SSA based on the SPI (Rivera 2014), larger NDE with shorter MDD were identified considering meteorological droughts, i.e., based solely on precipitation data. This indicates that not all meteorological

drought events will eventually lead to streamflow drought conditions, as suggested by Wong et al. (2013). Moreover, streamflow droughts have longer mean duration than meteorological droughts, due to the combined effect of pooling and lengthening (Hisdal and Tallaksen 2003).

3.3 Temporal evolution of streamflow droughts

The amount of stations with SHDI values corresponding to streamflow drought conditions can be used to quantify the spatial extension of drought events. In this sense, Fig. 5 shows the temporal evolution of the stations with $SHDI \leq -1.0$ on a monthly basis during 1961–2006. A clustering of the dry periods is evident during the 1960s until 1973, with the largest spatial extension of streamflow drought conditions recorded between 1968 and 1970. The highest amount of affected stations of the whole period was recorded in June 1968, with 38 stations with streamflow drought conditions, 23 of them under

Fig. 4 SHDI time series of de los Patos river at Álvarez Condarco (station 15) and Uruguay river at Paso de los Libres (station 46)

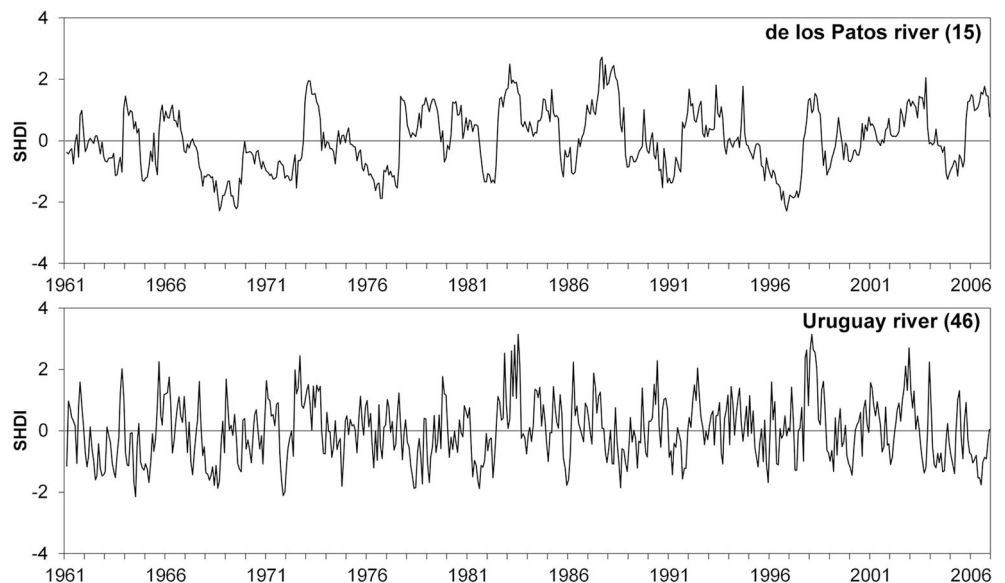
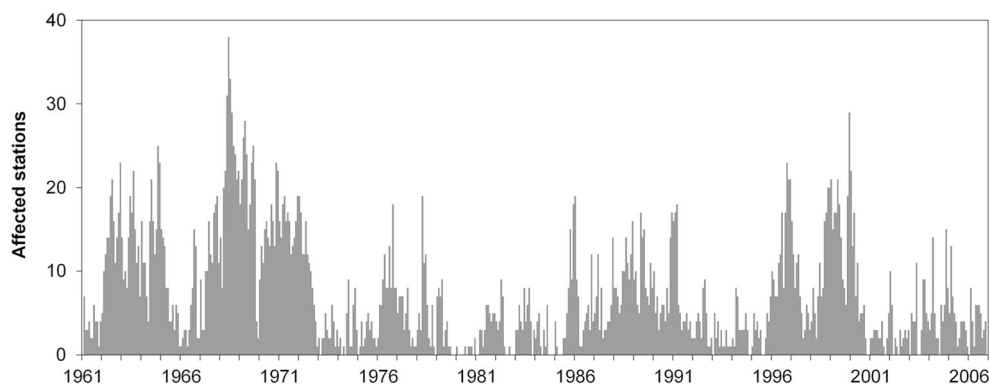


Fig. 5 Monthly evolution of the stations affected by streamflow drought conditions ($\text{SHDI} \leq -1.0$)



severe drought conditions. Moreover, 13 stations reached extreme drought conditions during October 1968 (not shown). Other relevant dry periods were recorded during the second half of 1980 decade and between 1996 and 2001, being December of 1999 the second month with the largest amount of affected stations (29 stations, 11 under severe streamflow drought conditions). The spatial extension of streamflow droughts was considerably higher during the 1960s, with 25 months from a total of 34 months (1961–2006) with at least 20 stations under drought conditions. This result resembles the spatial pattern identified by Rivera and Penalba (2014) considering the percentage of meteorological stations affected by drought conditions ($\text{SPI} \leq -1.0$).

The monthly sum of simultaneously affected stations enables the identification of the large events and their durations, but does not show the regional patterns of streamflow drought and its severity. The spatial extension of the drought periods recorded in June 1968 and December 1999 is shown in Fig. 6 to exemplify the regional drought patterns and its severity during the two most widespread drought months. During June 1968, only three stations reached extreme streamflow drought conditions, located over Southern LPB; nevertheless, 23 stations reached severe conditions, distributed along most of the analyzed basins. Particularly, the stations from Colorado Basin recorded prolonged drought conditions during the years 1967 to 1971 due to a lack of snowfall over the Central Andes (Rivera et al. 2017a). The spatial distribution of stations with streamflow drought conditions during December 1999 shows that the affected basins are located mostly over Patagonia and LPB (Fig. 6). Most of the stations of Colorado Basin recorded mild drought conditions, not reaching the threshold selected to define drought conditions. Stations under severe drought conditions are located mostly over Patagonia, where the large annual number of days with low streamflows was recorded during 1999 (Rivera et al. 2017b) and hydropower generation was largely affected. Dry conditions over most of LPB was associated to the occurrence of one of the largest La Niña event of the

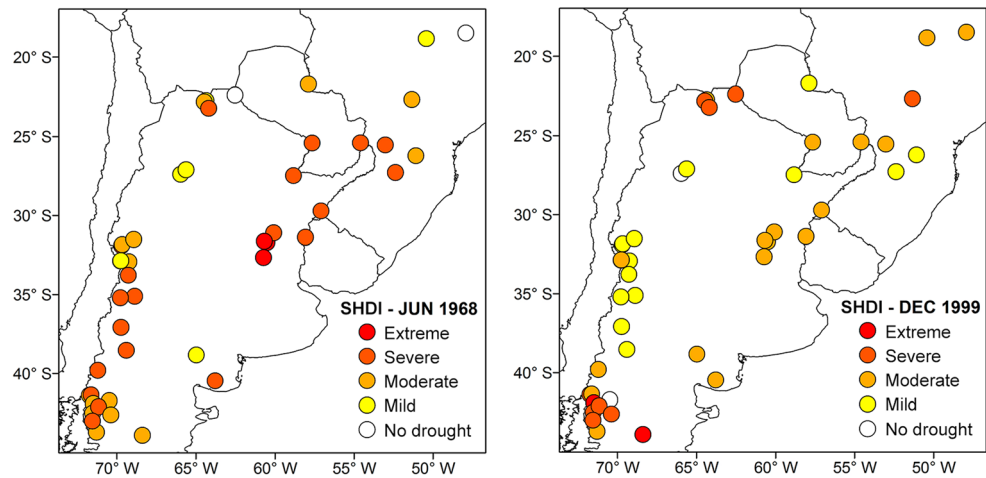
century that lead to a precipitation decrease over the region (Zanvettor and Ravelo 2000).

Regarding trends in the SHDI time series, Fig. 7 shows that the majority of the stations presented positive trends, most of them significant at a 99% confidence. Trends are in line with precipitation increases over SSA, specially during the 1980s and 1990s, as a consequence of an increase in regional precipitation due to a large number of El Niño years in comparison with the 1960s and 1970s (Penalba and Rivera 2016) and a decrease in the mean meridional gradient of temperature, which implies a displacement to higher latitudes of the Atlantic Subtropical High (Barros et al. 2000). Moreover, part of these trends can be attributed to land use change over LPB since 1970, as shown previously by Doyle and Barros (2011). As a result of the SHDI trends, an increase in the hydropower generation was evident since 1970s in all the countries of SSA. Negative trends in the SHDI are confined mostly to the Patagonian basins (Pacific and Atlantic basins, Negro Basin, and Central Patagonia basins). These trends can be linked with the trend towards a positive phase of the Southern Annular Mode (SAM, Marshall 2003). This pattern led to an increase in the pressure in mid-latitudes (around 40°S) and a decrease in the pressure at high latitudes (around 65°S). The trend in the SAM is associated with a southward shift in the storm tracks, which led to a decrease in the number of cyclones over the Southern Hemisphere and a rainfall decrease, i.e., leading to more frequent streamflow drought conditions.

4 Conclusions and discussion

This work analyzed the statistical properties of the streamflows over Southern South America (18°S to 50°S) in terms of the occurrences of streamflow droughts, using the Standardized Streamflow Index as a drought indicator over 46 monthly streamflow time series covering 46 years (1961–2006). The SHDI was selected given that it is a natural extension of the well-known SPI, retaining its advantages in terms of simplicity, based only on streamflow data, and versatility

Fig. 6 Spatial distribution of the streamflow drought categories during June 1968 (*left*) and December 1999 (*right*)



can be calculated on any time scale. Another key advantage is that SHDI and SPI are similar which eases the conjunctive analysis of meteorological and hydrological droughts (Dehghani et al. 2014). Previous studies over SSA typically used streamflow anomalies (Scarpati et al. 2001; Compagnucci and Araneo 2005), streamflow expressed as percentage deviations from the mean (Kane 2005) or the threshold level methodology on yearly (Fernández-Larrañaga 1997; Fernández and Buscemi 2000; Díaz et al. 2016) and daily basis (Vich et al. 2010; Rivera et al. 2017a, b) to analyze streamflow drought conditions. In this sense, besides local studies (Núñez et al. 2014 and Rangelcroft et al. 2016 in north-central Chile; Bianchi et al. 2017 in central-western Argentina), the use of standardized indices as a regional streamflow drought indicators is novel over SSA.

The initial—and probably most relevant—step in the calculation of the SHDI is to select a probability distribution that fits in a proper way the monthly streamflow records, as selection of an inappropriate distribution can impart bias to the index values, exaggerating or minimizing drought severity (Sienz et al. 2012). Recent papers focused on comparing different distributions for typical standardized drought indices like SPI, the Standardized Precipitation-Evapotranspiration Index (SPEI) or the SSI (Vicente-Serrano et al. 2012; Blain and Meschiatti 2015; Stagge et al. 2015). Considering that a probability distribution is no more than an approximation to the observed streamflow data, this study selected the GA probability distribution to fit the monthly streamflow records over SSA. We verified its suitability by using the AD test, one of the most rigorous and sensitive goodness-of-fit tests to deal with drought assessments. As an additional requirement, we considered that significant fits are mandatory in 8 out of 12 months of the year in order to consider the GA distribution as a proper option. Moreover, after the transformation of the typically highly skewed distribution of monthly streamflows into the standard normal distribution, we analyzed if the GA distribution leads to normally distributed SHDI time series. From an initial database of 53 stations, the records from 7 of them were discarded, obtaining a total of 87% of significant fits that proves the suitability of the GA distribution to represent monthly streamflows over SSA. It must be considered that this study was performed considering the SHDI on time scale of 1 month, i.e., no accumulation of streamflow records. With longer accumulation periods, the Central Limit Theorem states that the GA distribution should eventually approach a normal distribution (Stagge et al. 2015), leading to a probable increase in the significant fits when considering typical time scales of accumulation (3, 6, or 12 months), as it was verified with the SPI (Rivera 2014). A similar percentage of acceptances was observed in the case of the normality of the SHDI series, confirming its appropriateness to quantify streamflow drought conditions.

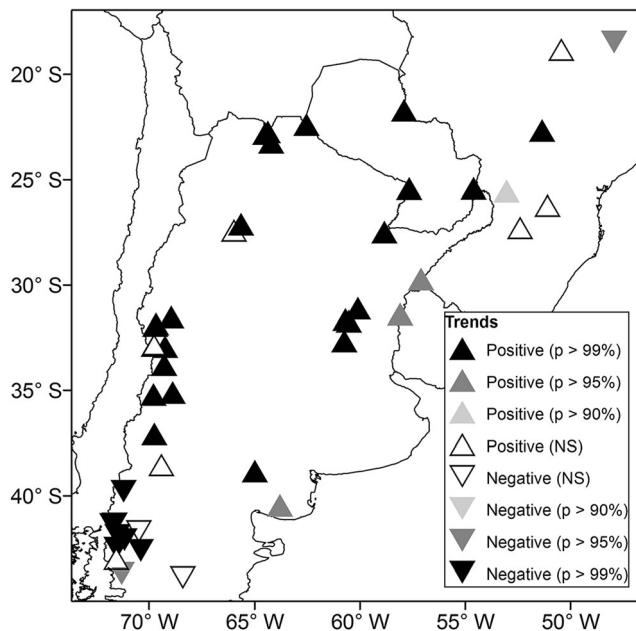


Fig. 7 Spatial distribution of the SHDI trends during the period 1961–2006

Based on the final 46 SHDI time series, we obtained the main characteristics of streamflow droughts—number of drought events, mean duration, and mean severity—over the 1961–2006 period. We found that drought frequency is related to its duration, given that the basins with more (less) number of streamflow drought events have short (large) mean duration. This relationship is an indicator of the different temporal variabilities that modulate the SHDI time series across SSA, arising from the different climatic features of the study area. Low frequency variations are evident in regions where snow-melt contributes significantly to monthly streamflow totals, while high frequency variations are relevant in regions where several synoptic factors affect the annual cycle of precipitation and its signal in streamflows. These factors are relevant and need to be considered for a proper regional monitoring of streamflow droughts. In the case of the severity, we found a regional pattern that is not related with drought frequency or its mean duration, leading to hypothesize that the role of the catchment characteristics is relevant in modulating the drought intensity.

There has been relatively limited research on the spatial aspects of hydrological drought (Van Loon 2015). Our results show that the spatial pattern of streamflow drought characteristics is not homogeneous, as observed by comparing two of the months with the higher number of affected stations (June 1968 with 38 affected stations and December 1999 with 29 affected stations, Fig. 6). For example, just in 6% of the time, more than 20 stations were affected simultaneously by streamflow drought conditions of different severity levels, mostly between 1961 and 1972. This highlights that widespread streamflow drought conditions are not a typical feature over SSA. In comparison with meteorological drought characteristics, this work showed that streamflow droughts are less regionally homogeneous, less frequent, and last for longer time periods than precipitation droughts based on SPI, a result that is in line with previous findings in Europe (Hisdal and Tallaksen 2003). This may be associated to the role of the catchment characteristics in the modulation of the drought signal from the meteorological to the hydrological deficits, a topic that deserves further research.

Observed trends in SHDI time series are in line with precipitation trends, being negative over the headwaters of Patagonian basins and positive in the rest of the basins. Mechanisms that contributed to the observed trends in precipitation are mainly associated to the observed trend towards a positive phase of the SAM that resulted in a decrease in precipitation totals over western Patagonia (Rivera et al. 2017b), an increase in the annual snow water equivalent after 1977/78 in the headwaters of Colorado Basin as a result of more recurrent El Niño events (Masiokas et al. 2006) that also influenced precipitation patterns over LPB (Barros and Silvestri 2002) leading to an increase in precipitation totals. Nevertheless, there is a strong non-linear variability in the

hydrometeorological trends over SSA, evident in both streamflow and precipitation records, that is indicative of a low-frequency climatic oscillation that modulates the regional aspects of precipitation in SSA (Rivera and Penalba 2014). This non-linearity must be considered in regional streamflow drought monitoring, together with the streamflow drought characteristics, for an improvement in water use practices and policies over SSA. The analysis presented in this paper generated baseline information for climate modeling studies at basin level, for the assessment of the impact of global warming in future drought characteristics and for water managers and policymakers as reference to the development of regional drought mitigation strategies.

Acknowledgements This work was supported by the University of Buenos Aires under grant UBA-20020130100263BA and the Argentinean Council of Research and Technology (CONICET) under grant PIP 11220150100137CO. We thank the Subsecretaría de Recursos Hídricos de Argentina for providing the monthly streamflow data used in the study.

References

- Alexandersson H (1986) A homogeneity test applied to precipitation data. *J Climatol* 6:661–675
- Amor LG, Carrasco A, Ibáñez JC (2009) Using and testing drought indicators. In: Iglesias A, Garrote L, Cancelliere A, Cubillo F, Willite D (eds) Coping with drought risk in agriculture and water supply systems. Drought Management and Policy Development in the Mediterranean. Springer Netherlands, Dordrecht, pp 55–65
- Anderson TW, Darling DA (1952) Asymptotic theory of certain “goodness of fit” criteria based on stochastic processes. *Ann Math Stat* 23:193–212
- Andreadis KM, Lettenmaier DP (2006) Trends in 20th century drought over the continental United States. *Geophys Res Lett* 33:L10403. doi:10.1029/2006GL025711
- Barker LJ, Hannaford J, Chiveron A, Svensson C (2016) From meteorological to hydrological drought using standardised indicators. *Hydrol Earth Syst Sci* 20:2483–2505
- Barros V, Silvestri GE (2002) The relation between sea surface temperature at the subtropical south-central Pacific and precipitation in southeastern South America. *J Clim* 15:251–267
- Barros VR, Castañeda ME, Doyle ME (2000) Recent precipitation trends in southern South America East of the Andes: an indication of a mode of climatic variability. In: Smolka PP, Volkheimer W (eds) Southern hemisphere paleo and neoclimates. Springer Berlin Heidelberg, New York, pp 187–206
- Bianchi L, Rivera J, Rojas J, Britos Navarro M, Villalba R (2017) A regional water balance indicator inferred from satellite images of an Andean endorheic basin in central-western Argentina. *Hydrol Sci J* 62(4):533–545
- Blain GC, Meschiatti MC (2015) Inadequacy of the gamma distribution to calculate the Standardized Precipitation Index. *Revista Brasileira de Engenharia Agrícola e Ambiental* 19(12):1129–1135
- Carril AF, Cavalcanti IFA, Menéndez CG, Sörensson A, López-Franca N, Rivera JA, Robledo F, Zaninelli PG, Ambrizzi T, Penalba OC, da Rocha RP, Sánchez E, Bettolli ML, Pessag N, Renom M, Ruscica R, Solman S, Tencer B, Grimm A, Rusticucci M, Cherchi A, Tedeschi R, Zamboni L (2016) Extreme events in La Plata basin: a

- retrospective analysis of what we have learned during CLARIS-LPB project. *Clim Res* 68:95–116
- Cavalcanti IFA, Carril A, Penalba O, Grimm AM, Menendez C, Sánchez E, Cherchi A, Sörensson A, Robledo F, Rivera J, Pántano V, Bettolli ML, Zaninelli P, Zamboni L, Tedeschi RG, Dominguez M, Ruscica R, Flach R (2015) Precipitation extremes over La Plata Basin—review and new results from observations and climate simulations. *J Hydrol* 523:211–230
- Compagnucci RH, Araneo DC (2005) Identificación de áreas de homogeneidad estadística para los caudales de ríos andinos argentinos y su relación con la circulación atmosférica y la temperatura superficial del mar. *Meteor-Forschung* 30(1–2):41–53
- Cuya DGP, Brandimarte L, Popescu I, Alterach J, Peviani M (2013) A GIS-based assessment of maximum potential hydropower production in La Plata Basin under global changes. *Renew Energy* 50:103–114
- Dehghani M, Saghafian B, Nasiri Saleh F, Farokhnia A, Noori R (2014) Uncertainty analysis of streamflow drought forecast using artificial neural networks and Monte-Carlo simulation. *Int J Climatol* 34:1169–1180
- Díaz E, Rodríguez A, Dölling O, Bertoni JC, Smrekar M (2016) Identificación y caracterización de sequías hidrológicas en Argentina. *Tecnología y Ciencias del Agua* 7(1):125–133
- Doyle ME, Barros VR (2011) Attribution of the river flow growth in the Plata Basin. *Int J Climatol* 31:2234–2248
- Fernández HW, Buscemi NH (2000) Análisis y caracterización de sequías hidrológicas en el Centro Oeste de Argentina. In: Proceedings of the XVIII Congreso Nacional del Agua (CONAGUA). Universidad Nacional de Santiago del Estero, Termas de Río Hondo, CD-ROM
- Fernández-Larrañaga B (1997) Identificación y caracterización de sequías hidrológicas en Chile Central. *Ingeniería del Agua* 4(4):37–46
- Feyen L, Dankers R (2009) Impact of global warming on streamflow drought in Europe. *J Geophys Res* 114:D17116. doi:10.1029/2008JD011438
- Gan M, Rao V (1991) Surface cyclogenesis over South America. *Mon Wea Rev* 119:1293–1302
- Garreaud RD, Vuille M, Compagnucci R, Marengo J (2009) Present-day South American climate. *Palaeogeogr Palaeoclimatol Palaeoecol* 281:180–195
- Hamed KH, Rao AR (1998) A modified Mann-Kendall trend test for autocorrelated data. *J Hydrol* 204(1–4):182–196
- Hayes M, Svoboda M, Wall N, Widham M (2011) The Lincoln declaration on drought indices: universal meteorological drought index recommended. *Bull Am Meteorol Soc* 92(4):485–488
- Heim RR (2002) A review of twentieth century drought indices used in the United States. *Bull Am Meteorol Soc* 83:1149–1165
- Hisdal H, Tallaksen L (2003) Estimation of regional meteorological and hydrological drought characteristics: a case study for Denmark. *J Hydrol* 281:230–247
- Kane RP (2005) Spectral characteristics and ENSO relationship of the Paraná river streamflow. *Mausam* 56(2):367–374
- Khaliq MN, Ouarda TBMJ, Gachon P (2009) Identification of temporal trends in annual and seasonal low flows occurring in Canadian rivers: the effect of short- and long-term persistence. *J Hydrol* 369:183–197
- Kulkarni A, Von Storch H (1995) Monte-Carlo experiments on the effect of serial correlation on the Mann-Kendall test for trend. *Meteorol Z* 4(2):82–85
- Laio F (2004) Cramer–von Mises and Anderson-Darling goodness of fit tests for extreme value distributions with unknown parameters. *Water Resour Res* 40:W09308. doi:10.1029/2004WR003204
- Lloyd-Hughes B, Saunders MA (2002) A drought climatology for Europe. *Int J Climatol* 22(13):1571–1592
- Marshall GJ (2003) Trends in the southern annular mode from observations and Reanalyses. *J Clim* 16:4134–4143
- Masiokas M, Villalba R, Luckman B, Le Quesne C, Aravena JC (2006) Snowpack variations in the Central Andes of Argentina and Chile, 1951–2005: large-scale atmospheric influences and implications for water resources in the region. *J Clim* 19:6334–6352
- McKee TB, Doesken NJ, Kleist J (1993) The relationship of drought frequency and duration to time scales. In: Proceedings of the Eight Conference on Applied Climatology. American Meteorological Society, Anaheim, pp 179–184
- Nalbantis I, Tsakiris G (2009) Assessment of hydrological drought revisited. *Water Resour Manag* 23:881–897
- Núñez J, Rivera D, Oyarzún R, Arumí JL (2014) On the use of standardized drought indices under decadal climate variability: critical assessment and drought policy implications. *J Hydrol* 517:458–470
- Penalba OC, Rivera JA (2013) Future changes in drought characteristics over southern South America projected by a CMIP5 ensemble. *Am J Clim Chang* 2(3):173–182
- Penalba OC, Rivera JA (2016) Precipitation response to El Niño/La Niña events in Southern South America—emphasis in regional drought occurrences. *Adv Geosci* 42:1–14
- Penalba OC, Rivera JA, Pántano VC (2014) The CLARIS LPB database: constructing a long-term daily hydro-meteorological dataset for La Plata Basin, Southern South America. *Geosci Data J* 1:20–29
- Rangecroft S, Van Loon AF, Maureira H, Verbist K, Hannah DM (2016) Multi-method assessment of reservoir effects on hydrological droughts in an arid region. *Earth Syst Dynam Discuss*. doi:10.5194/esd-2016-57
- Rivera JA (2014) Aspectos climatológicos de las sequías meteorológicas en el sur de Sudamérica. Análisis regional y proyecciones futuras. University of Buenos Aires. http://digital.bl.fcen.uba.ar/Download/Tesis/Tesis_5504_Rivera.pdf. Accessed 7 October 2016
- Rivera JA, Penalba OC (2014) Trends and spatial patterns of drought affected area in southern South America. *Climate* 2:264–278
- Rivera JA, Araneo DC, Penalba OC (2017a) Threshold level approach for streamflow droughts analysis in the Central Andes of Argentina: a climatological assessment. *Hydrol Sci J* (in press)
- Rivera JA, Araneo DC, Penalba OC, Villalba R (2017b) Regional aspects of streamflow droughts in the Andean rivers of Patagonia, Argentina Links with large-scale climatic oscillations *Hydrology Research*. doi:10.2166/nh.2017.207
- Scarpati OE, Spescha L, Fioriti MJ, Capriolo AD (2001) El Niño driven climate variability and drainage anomalies in Patagonian region, Argentina. *Cuadernos de Investigación Geográfica* 27:179–191
- Shiferaw B, Tesfaye K, Kassie M, Abate T, Prasanna BM, Menkir A (2014) Managing vulnerability to drought and enhancing livelihood resilience in sub-Saharan Africa: technological, institutional and policy options. *Weather and Climate Extremes* 3:67–79
- Shin H, Jung Y, Jeong C, Heo J-H (2012) Assessment of modified Anderson–Darling test statistics for the generalized extreme value and generalized logistic distributions. *Stoch Environ Res Risk Assess* 26:105–114
- Shukla S, Wood AW (2008) Use of a standardized runoff index for characterizing hydrologic drought. *Geophys Res Lett* 35:L02405. doi:10.1029/2007GL032487
- Siens F, Bothe O, Fraedrich K (2012) Monitoring and quantifying future climate projections of dryness and wetness extremes: SPI bias. *Hydrol Earth Syst Sci* 16:2143–2157
- Soláková T, De Michele C, Vezzoli R (2014) Comparison between parametric and nonparametric approaches for the calculation of two drought indices: SPI and SSI. *J Hydrol Eng* 19(9). doi:10.1061/(ASCE)HE.1943-5584.0000942
- Sousa PM, Trigo RM, Aizpurua P, Nieto R, Gimeno L, Garcia-Herrera R (2011) Trends and extremes of drought indices throughout the 20th century in the Mediterranean. *Nat Hazards Earth Syst Sci* 11:33–51
- Stagge JH, Tallaksen LM, Gudmundsson L, Van Loon AF, Stahl K (2015) Candidate distributions for climatological drought indices (SPI and SPEI). *Int J Climatol* 35(13):4027–4040

- Stephens MA (1976) Asymptotic power of EDF statistics for exponentiality against gamma and Weibull alternatives. Technical report no. 297, Department Statistic Stanford University
- Svensson C, Hannaford J, Prosdocimi I (2017) Statistical distributions for monthly aggregations of precipitation and streamflow in drought indicator applications. *Water Resour Res* 53. doi:10.1002/2016WR019276
- Tabari H, Nikbakht J, Talaee PH (2013) Hydrological drought assessment in northwestern Iran based on streamflow drought index (SDI). *Water Resour Manag* 27:137–151
- Van Loon AF (2015) Hydrological drought explained. *WIREs Water* 2015. doi:10.1002/wat2.1085
- Vera CS, Vigliarolo PK, Berbery EH (2002) Cold season synoptic scale waves over subtropical South America. *Mon Wea Rev* 130:684–699
- Vicente-Serrano SM, López-Moreno JJ, Beguería S, Lorenzo-Lacruz J, Azorin-Molina C, Morán-Tejada E (2012) Accurate computation of a streamflow drought index. *J Hydrol Eng* 17:318–332
- Vich A, Bizzotto F, Vaccarino E, Correas M, Manduca F (2010) Tendencias y cambios abruptos en el escurrimiento de algunos ríos con nacientes en la cordillera y serranías del oeste argentino. In: Paoli CU, Malinow GV (eds) *Criterios para la determinación de crecidas de diseño en sistemas climáticos cambiantes*. Universidad Nacional del Litoral, Santa Fe, pp 149–166
- Vich AJJ, Norte FA, Lauro C (2014) Análisis regional de frecuencias de caudales de ríos pertenecientes a cuencas con nacientes en la Cordillera de Los Andes. *Meteorologica* 39:3–26
- Wilhite DA, Sivakumar MVK, Pulwarty R (2014) Managing drought risk in a changing climate: the role of national drought policy. *Weather and Climate Extremes* 3:4–13
- Wong G, Van Lanen HAJ, Torfs PJJF (2013) Probabilistic analysis of hydrological drought characteristics using meteorological drought. *Hydrol Sci J* 58(2):253–270
- World Meteorological Organization (WMO) (2008) *Manual on Low-flow Estimation and Prediction*. WMO No. 1029, Geneva, Switzerland
- Wu H, Soh L-K., Samal A, Chen X-H (2007a) Trend analysis of streamflow drought events in Nebraska. *Water Resour Manag*, doi:10.1007/s11269-006-9148-6
- Wu H, Svoboda MD, Hayes MJ, Wilhite DA, Wen F (2007b) Appropriate application of the standardized precipitation index in arid locations and dry seasons. *Int J Climatol* 27:65–79
- Zanvettor R, Ravelo A (2000) Using the SPI to monitor the 1999-2000 drought in Northeastern Argentina. *Drought Network News* 12(3): 3–4
- Zhang Q, Li J, Singh VP, Bai Y (2012) SPI-based evaluation of drought events in Xinjiang, China. *Nat Hazards* 64:481–492
- Zhu Y, Chang J, Huang S, Huang Q (2016) Characteristics of integrated droughts based on a nonparametric standardized drought index in the Yellow River Basin, China. *Hydrol Res* 47(2):454–467